Photoemission of spin-polarized electrons from GaAs

Daniel T. Pierce* and Felix Meier
Laboratorium für Festkörperphysik, Eidgenössische Technische Hochschule, CH 8049, Zürich, Switzerland
(Received 10 February 1976)

The spin polarization of electrons photoemitted from (110) GaAs by irradiating with circularly polarized light of energy $1.5 < \hbar\omega < 3.6$ eV was measured by Mott scattering. The GaAs surface was treated with cesium and oxygen to obtain a negative electron affinity (NEA). The spectrum of spin polarization $P(\hbar\omega)$ exhibits a peak ($P = 40\%$) at threshold arising from transitions at Γ, and positive ($P = 8\%$) and negative ($P = -8\%$) peaks at 3.0 and 3.2 eV, respectively, arising from transitions at L (Λ). Anomalous behavior, consisting of a depolarization at threshold and an increase and shift in the peak polarization to 54% at 1.7 eV, is attributed to a small positive electron affinity (PEA) characteristic of some samples. Restriction of the photoelectron emission angle by the PEA leads directly to the anomalously high P. Results of calculations show that P cannot be increased above 50% for emission arising from transitions at Γ in NEA GaAs. Our detailed interpretation of the spectra indicates how spin-polarized photoemission can be used to study the spin-dependent aspects of electronic structure. The outstanding qualities of NEA GaAs as a source of spin-polarized electrons are discussed and compared with other sources.

I. INTRODUCTION

In recent years, spin-polarized photoemission measurements have proven to be very valuable in studying magnetically ordered materials.[1] In this paper we present an in-depth discussion of the first measurements of spin-polarized photoelectrons from a semiconductor which is not magnetically ordered. We have previously given brief reports of our measurements of GaAs which show (i) the value of spin-polarized photoemission as a probe of the spin-dependent electronic structure of a nonmagnetic material[2] and (ii) the potential of negative-electron-affinity (NEA) GaAs as a *source* of spin-polarized electrons.[3]

An overview of the principles of spin-polarized photoemission measurements of nonmagnetic materials is given in Sec. II. Basic symmetry considerations provide a framework for comparing polarized photoemission measurements from materials with and without magnetic order. The spin polarization is created in the nonmagnetic material in the optical excitation process as a result of the selection rules for transitions produced by circularly polarized light. By appropriate surface treatment, the vacuum level of GaAs can be lowered so that even electrons at the conduction-band minimum can be emitted. The polarization of the photoemitted electrons may be less than that calculated from the selection rules if there is spin relaxation during the emission process. The experimental procedures specific to the results of this work are discussed in Sec. III.

In Sec. IV we discuss the measured photoelectric yield and the spectrum of spin polarization $P(\hbar\omega)$. Spectra of spin polarization from nonmagnetic materials exhibit structure due to the spin-orbit splitting of the electron energy bands. The spectrum from GaAs can be understood in detail in terms of the band structure of GaAs, which is well known. From this example, we see the kind of new information we could obtain from a less well known material. For GaAs, we find a high P of 40% at threshold, $\hbar\omega \sim 1.5$ eV, due to transitions at Γ. P decreases for excitations away from $k = 0$ at slightly higher $\hbar\omega$ owing to the changing of the wave functions, particularly for electrons in the light-hole band. As the photon energy is increased above the onset of emission from the spin-orbit split-off band, P gradually decreases to zero.

Two anomalous spectra exhibited a low polarization at threshold, a shift in the position of the maximum P to $\hbar\omega = 1.7$ eV, and an increase in the maximum P to 54%. These phenomena can be explained by assuming that a small positive electron affinity (PEA) was obtained for these samples. We show that when the emission of the electrons is confined to a cone about the surface normal and light direction, as in the case of a PEA surface, a polarization greater than the NEA theoretical maximum of 50% is possible. The calculation also shows that the maximum P to be expected from an NEA surface if 50% even if it were possible to isolate transitions from the heavy-hole band.

Transitions of [111] symmetry (L, Λ) give rise to a positive and negative peak each with $P \sim 8\%$ at $\hbar\omega = 3.0$ and 3.2 eV, respectively. The difference between the shape of structure in the spectrum due to these transitions and those at Γ is explained by the relatively parallel energy bands near L (Λ). Because of the anisotropy of the excitation and of the direct emission at L, it is expected that the

polarization due to these transitions depends on the crystal face from which the emission is observed. Thermalization of excited electrons into L or X minima as well as intervalley scattering change the polarization from that calculated for direct emission.

A good source of spin-polarized electrons has been sought for many years. The use of NEA GaAs as a source of polarized electrons has been proposed previously.[4] In Sec. V we describe briefly the criteria for a good source of polarized electrons and discuss NEA GaAs in light of them. The GaAs source is then compared to the best other sources of polarized electrons currently available. It is seen that the GaAs source combines simplicity with unmatched efficiency.

II. PRINCIPLE OF THE EXPERIMENT

A. Symmetry considerations

A simplified schematic diagram of the spin-polarized photoemission experiment is shown in Fig. 1. Light of photon energy $\hbar\omega$ impinges on the sample surface, and electrons are photoemitted. Instead of measuring the intensity of emission as a function of electron kinetic energy as in conventional photoemission experiments, we measure the electron spin polarization, typically as a function of photon energy. The electron spin polarization is defined as

$$P=\frac{N\uparrow - N\downarrow}{N\uparrow + N\downarrow}\,, \tag{1}$$

where $N\uparrow(N\downarrow)$ are the numbers of electron magnetic moments parallel (anti parallel) to a preferred direction.

The spin, like an angular momentum $\vec{L}=\vec{r}\times\vec{p}$, is an axial vector which does not change sign under a parity operation ($x\to -x$, $y\to -y$, $z\to -z$). A quantity which produces a spin polarization or which defines a preferred direction with respect to which P is measured as in Eq. (1), must therefore be an axial vector also. In the case of a magnetically ordered material, such as ferromagnetic Fe, the magnetization $\vec{M}$ specifies the polarization. Experimentally a magnetic field $\vec{H}$ is applied to align the domains and determine the direction of $\vec{M}$. In the case of a nonmagnetic solid, the electrons are oriented in the optical excitation process with circularly polarized light. The preferred direction is given by the *angular momentum* of the *circularly polarized* light.

The polarization is measured by Mott scattering as indicated schematically in Fig. 1. The longitudinal polarization (P along the electron momentum) is changed to a transverse polarization by a 90° deflection of the beam. The electrons are then accelerated to 100 keV and scattered from a thin gold foil. The scattering cross section depends on the spin direction with respect to the normal $\hat{n}$ to the scattering plane,

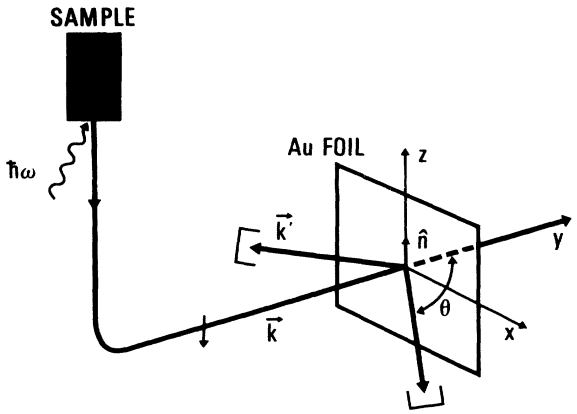

FIG. 1. Schematic of the spin-polarized photoemission experiment showing the light $\hbar\omega$ incident on the sample giving rise to a longitudinally polarized beam which is transported by electron optics, deflected 90° to obtain a transverse polarization, and accelerated to 100 keV for Mott scattering from the Au foil. The left-right scattering asymmetry gives a measure of the polarization.

$$\sigma(\theta)=\sigma_0(\theta)[1+S(\theta)\vec{P}\cdot\hat{n}]\,, \tag{2}$$

where $\hat{n}=\vec{k}\times\vec{k}'/|\vec{k}\times\vec{k}'|$ is an axial vector as required; $\vec{k}$ and $\vec{k}'$ are the wave vectors of the incident and scattered electrons, respectively. The left-right asymmetry in the scattering arises from the interaction of the electron spin with its orbital angular momentum as it scatters from the gold nucleus. The degree of scattering asymmetry is given by the Sherman function,[5] $S(\theta)$, where $S(\theta)=0.39$ for scattering of 100-keV electrons at $\theta=120°$ from an infinitely thin gold foil.

B. Optical orientation of spins

In atomic physics, the orientation of electron magnetic moments by means of irradiation with light of suitable polarization has been used for a long time.[6] One distinguishes between orientation in the excited state and orientation in the ground state. Sometimes only the latter is called "optical pumping". In our experiment, we use this term for the orientation of the magnetic moments in the excited state.

An overpopulation of a certain spin direction in the excited state can be achieved by making use of the combined effects of selection rules and intensity ratios of the various energetically possible transitions. For an atom, owing to its full rota-

tional symmetry, these quantities can be calculated in a reasonably straightforward manner. In a solid, where the wave functions are assumed to be of the form $\Phi_k = u_k e^{i\vec{k}\cdot\vec{r}}$ the problem is generally much more difficult. However, at certain points of the Brillouin zone it is still possible to get a clear picture of the transition processes, as will be seen from our discussion of GaAs.

GaAs has the zinc-blende structure, in which the lattice consists of two interpenetrating fcc lattices, one occupied by Ga and the other by As ions. We know from experiment and band-structure calculations for GaAs that the wave functions at the valence-band maximum and conduction-band minimum have p and s symmetry, respectively. At Γ, where k is zero, the symmetry of the point group is not reduced. In particular, for a cubic crystal the p levels at Γ are not split by the crystal field.[7]

What is absolutely essential for the optical pumping process is that the spin-orbit interaction *does* split the sixfold degenerate p band at Γ into a fourfold degenerate $P_{3/2}$ level and twofold degenerate $P_{1/2}$ level which lies $\Delta = 0.34$ eV lower than $P_{3/2}$.[8] Figure 2 shows the energy bands at Γ on the left and the degenerate states labeled by their m_j quantum numbers on the right along with the relevant transition probabilities.

A second very important fact is that GaAs is a direct-gap semiconductor with the minimum band separation E_g at Γ. Therefore, when $\hbar\omega \gtrsim E_g$, only transitions between states of well-defined angular momentum, characteristic of Γ, are induced. Other transitions are energetically impossible.

The production of spin-oriented electrons in the conduction band occurs as follows. Consider the case in which the sample is irradiated with σ^+ circularly polarized light[9] (light angular momentum in light direction $\vec{k}$). From the selection rule, only transitions with $\Delta m_j = m_f - m_i = 1$ are allowed; the angular momentum of the light defines the quantization axis. For light of energy $\hbar\omega \sim E_g$, the allowed transitions are from $m_j = -\frac{3}{2}$ (valence band) to $m_j = -\frac{1}{2}$ (conduction band) and from $m_j = -\frac{1}{2}$ to $m_j = +\frac{1}{2}$. The net polarization is given by the transition probabilities of these two transitions.

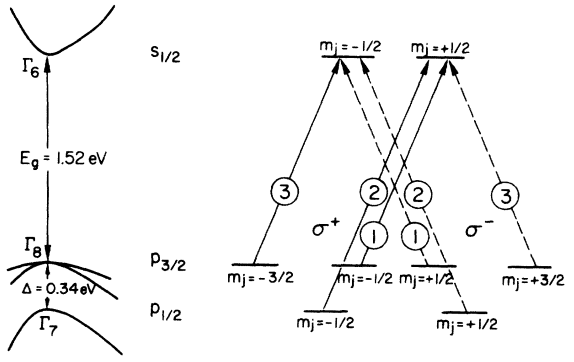

FIG. 2. On the left, an E-vs-k diagram of the energy bands of GaAs near $k = 0$ shows the energy gap E_g and the spin-orbit splitting Δ of the valence bands. The degenerate states at $k = 0$ are labeled on the right by their m_J quantum numbers. The allowed transitions for σ^+ ($\Delta m_j = 1$) and σ^- ($\Delta m_j = -1$) circularly polarized light are shown by the solid and dashed lines, respectively. The circles numbers represent the relative transition probabilities.

The relative transition probabilities can be obtained by calculating the matrix element of the transition $\langle \Psi_f | H_{\text{int}} | \Psi_i \rangle$, where $H_{\text{int}} \propto X \pm iY$ for $\sigma^\pm$ light. The angular and spin part of the wave function[10] is given for each state in Table I. The radial part of the wave function enters our calculation in ratios of radial matrix elements which cancel. The wave functions can be written in terms of the spherical harmonics Y_{lm} by replacing $(X+iY)/\sqrt{2}$, $(X-iY)\sqrt{2}$, and Z by $Y_{1,1}$, $-Y_{1,1}$, and $-Y_{1,0}$, respectively, again ignoring the factors of r. Writing the wave functions in terms of the spherical harmonics, we easily find that

$$\frac{|\langle \frac{1}{2}, -\frac{1}{2} | Y_{1,1} | \frac{3}{2}, -\frac{3}{2} \rangle|^2}{|\langle \frac{1}{2}, \frac{1}{2} | Y_{1,1} | \frac{3}{2}, -\frac{1}{2} \rangle|^2} = 3 \,. \tag{3}$$

Note that the electron spin does not change in the transition. As the photon energy is increased so that transitions are possible from the split-off valence band, for example, from $|\frac{1}{2}, -\frac{1}{2}\rangle$ to $|\frac{1}{2}, \frac{1}{2}\rangle$ with σ^+ light, P decreases to zero since these transitions come in with a relative intensity of 2. A more detailed discussion of the spectral variation of the polarization is given in Sec. IV, where the experimental results are discussed.

Away from the center of the Brillouin zone, the wave-function symmetry is determined by the

TABLE I. Angular and spin part of the wave function at Γ.

Symmetry point	$\lvert J, m_j \rangle$	Wave function
Γ_6	$\lvert \frac{1}{2}, \frac{1}{2} \rangle$	$\lvert S\uparrow \rangle$
	$\lvert \frac{1}{2}, -\frac{1}{2} \rangle$	$\lvert S\downarrow \rangle$
Γ_7	$\lvert \frac{1}{2}, \frac{1}{2} \rangle$	$\lvert -(\frac{1}{3})^{1/2}(X+iY)\downarrow - (\frac{1}{3})^{1/2} Z\uparrow \rangle$
	$\lvert \frac{1}{2}, -\frac{1}{2} \rangle$	$\lvert (\frac{1}{3})^{1/2}(X-iY)\uparrow - (\frac{1}{3})^{1/2} Z\downarrow \rangle$
Γ_8	$\lvert \frac{3}{2}, \frac{3}{2} \rangle$	$\lvert (\frac{1}{2})^{1/2}(X+iY)\uparrow \rangle$
	$\lvert \frac{3}{2}, \frac{1}{2} \rangle$	$\lvert -(\frac{1}{6})^{1/2}(X+iY)\downarrow + (\frac{2}{3})^{1/2} Z\uparrow \rangle$
	$\lvert \frac{3}{2}, -\frac{1}{2} \rangle$	$\lvert (\frac{1}{6})^{1/2}(X-iY)\uparrow + (\frac{2}{3})^{1/2} Z\downarrow \rangle$
	$\lvert \frac{3}{2}, -\frac{3}{2} \rangle$	$\lvert (\frac{1}{2})^{1/2}(X-iY)\downarrow \rangle$

point group of the crystal and the symmetry group of the k vector. At certain points on the surface of the Brillouin zone, symmetry-induced degeneracy of the energy levels is still possible. The spin-orbit splitting at the L point is observed in the spectra which are discussed in Sec. IV.

C. Lowering the vacuum level

Optical orientation of electron spins in the conduction band was first observed by Lampel[11] in 1968 by measuring the effect of the oriented carriers on the nuclear magnetization. Subsequently, orientation was detected by Parsons[12] for GaSb in a luminescence measurement. When the polarized electrons recombine, the emitted light is also polarized. Luminescence measurements of[13–18] GaAs substantiate the above analysis of the polarization at the Γ point. A recent review of the luminescence work has been given by Lampel.[19]

In contrast to the luminescence measurement, information about the electrons at the conduction-band minimum is not usually accessible in a photoemission measurement. Recall that the final state in the photoemission process must be above the vacuum level for the electron to be photoemitted. Fortuitously, in GaAs the electron affinity χ (the energy difference between the vacuum level and the conduction-band minimum in the bulk) can be decreased to zero and even made negative. While a negative electron affinity is not required for the observation of spin-dependent band structure at points other than the conduction-band minimum, it has important consequences for GaAs as a high-intensity source of spin-polarized electrons.

For a high-intensity source of photoelectrons, one wants to maximize the quantum efficiency or yield, defined as the average number of electrons photoemitted per incident photon of energy $\hbar\omega$. Scheer and van Laar[20] specified the band-structure properties of a high-yield photoemitter and showed that properly treated GaAs meets the requirements almost ideally. For maximum yield at low $\hbar\omega$, the photoemitter must have an energy gap E_g. In metals, photoexcited electrons of any energy can scatter inelastically with an electron below E_f to produce an electron-hole pair and lose sufficient energy so as not to be photoemitted. In a semiconductor on the other hand, an electron must be excited at least an energy E_g above the bottom of the conduction band ($\hbar\omega > 2E_g$) for pair production. For $\hbar\omega < 2E_g$ electron scattering with optical phonons still limits the the mean free path of the excited electron to the order of 100 Å. Since the penetration depth of the light is much greater than this, an excited electron can be scattered many times and lose sufficient energy so as to be below the vacuum level.

Clearly it is desirable to lower the vacuum level as far as possible. Scheer and van Laar found that it was possible to reduce the electron affinity from the ~4 eV of a clean GaAs surface [Fig. 3(a)] to about zero [Fig. 3(b)] by applying Cs to p-type GaAs. The Cs gives up an electron and a dipole layer is formed. If the GaAs surface is covered with layers of both cesium and oxygen, it is possible to achieve a negative electron affinity, as in Fig. 3(c). The nature of the Cs-O layer is a topic of current research.[21–23] It is believed that the activating layers have compositions on the Cs-rich side of the stoichiometric compound Cs_2O, which is a semiconductor. Depending on the degree of Cs excess, the activating layer ranges from a semiconductor which forms a heterojunction with the GaAs [as shown in Fig. 3(c)] to a metal which forms a Schottky barrier.[22] In the heterojunction activation mode, the relevant barrier is the heterojunction barrier, which remains 1.1 eV above the valence-band maximum.

The key feature of the NEA is that the photoelectron escape depth is now limited by the probability of recombination of the thermalized conduction electrons with valence-band holes. In other words, the escape depth corresponds to the diffusion length for thermalized electrons (~10^4Å) rather than to the hot-electron scattering length (~10^2Å). The photocurrent from an NEA emitter is therefore much larger than from the same emitter without NEA.

The art of activating GaAs photocathodes has

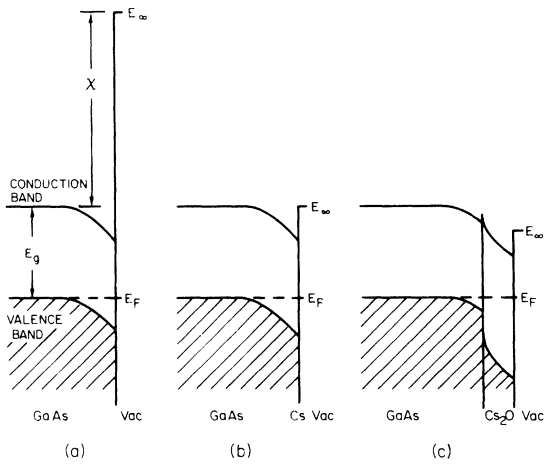

FIG. 3. Energy bands near the surface (E vs z) in p-type GaAs with different surface treatments: (a) clean GaAs with a high electron affinity; (b) GaAs with a layer of Cs, leading to an approximately zero electron affinity; and (c) GaAs with Cs-O treatment to produce a negative electron affinity.

been well developed.[24] Typically, the application of a Cs layer to the clean surface until the photocurrent is maximized is followed by alternate treatments of O and Cs [written hereafter as $(OCs)^n$]. A maximum escape probability has been reported for $n \simeq 5$ corresponding to a Cs-O layer ~10Å thick.[24]

D. Photoemission and spin relaxation

The degree of polarization of the photoemitted electrons may differ from the 50% value calculated in Sec. II B if the electrons undergo a spin-flip scattering process before being photoemitted. The spin-flip scattering processes determine a spin relaxation time τ_s. The average lifetime of the excited electrons in the bulk before photoemission is τ_{pe}. In the case of a negative-electron-affinity photoemitter, the electron recombination time τ_e determines the diffusion length and hence τ_{pe}. τ_s defines the decay of the difference in spin populations when the light is switched off:

$$\Delta N \equiv N\uparrow - N\downarrow = \Delta N_0 e^{-t/\tau_s} . \tag{4}$$

The total number of excited electrons N also decreases as the electrons are photoemitted or recombined:

$$N(t) = N_0 e^{-t/\tau_{pe}} . \tag{5}$$

The decay time τ of the magnetization $M_z = \mu(N\uparrow - N\downarrow) = \mu NP$ is seen from the time dependence of the magnetization

$$M(t) = M_0 e^{-t(1/\tau_s + 1/\tau_{pe})} \tag{6}$$

to be $\tau = \tau_s \tau_{pe}/(\tau_s + \tau_{pe})$.

Now for the case of equilibrium pumping conditions we have

$$\begin{aligned} \frac{dN\uparrow}{dt} &= C\uparrow - \frac{1}{2}\frac{N\uparrow - N\downarrow}{\tau_s} - \frac{N\uparrow}{\tau_e} = 0 , \\ \frac{dN\downarrow}{dt} &= C\downarrow - \frac{1}{2}\frac{N\downarrow - N\uparrow}{\tau_s} - \frac{N\downarrow}{\tau_e} = 0 , \end{aligned} \tag{7}$$

where $C\uparrow$, $C\downarrow$ are the production rates of $\uparrow$ and $\downarrow$ electrons. One obtains for the initial polarization P_0

$$\frac{C\uparrow - C\downarrow}{C\uparrow + C\downarrow} \equiv P_0 = \frac{(N\uparrow - N\downarrow)/\tau_s + (N\uparrow - N\downarrow)/\tau_e}{(N\uparrow + N\downarrow)/\tau_e} , \tag{8}$$

so that

$$P \equiv \frac{N\uparrow - N\downarrow}{N\uparrow + N\downarrow} = \frac{\tau_s}{\tau_{pe} + \tau_s} P_0 . \tag{9}$$

At this point one might be inclined to take the result of the experiment for granted since $\tau_{pe} < \tau_e$ (the electrons are emitted) and since from luminescence measurements we know that $\tau_e < \tau_s$. However, a word of caution is in order. We have not taken into consideration possible spin-flip scattering at the surface. If a fraction ζ of the up (down) spins is scattered into down (up) states, the measured polarization P_m is related to that in the bulk by

$$P_m = (1 - 2\zeta)P. \tag{10}$$

Previous work on cesiated Ni and Co showed that for cesium coverages from half to one monolayer the polarization at threshold decreased to zero.[25,26] It remains to measure what happens to the electrons photoemitted from GaAs as they pass through the Cs-O layer.

III. EXPERIMENTAL PROCEDURE

The measurement of electron-spin polarization by Mott scattering has been described in detail in earlier papers reporting results from magnetically ordered materials.[1,27–29] Here we discuss primarily the preparation of the GaAs sample, and the optics for the circularly polarized light, both of which differed from previous experiments. Figure 4 shows a schematic overview of the apparatus which consists of three main parts: (i) the sample preparation chamber, (ii) the photoemission chamber where the photoelectrons are also formed into a beam, and (iii) the 100-keV linear accelerator and Mott scatterer where the polarization is measured. The superconducting magnet (No. 4) was removed for these measurements. The cryostat was nevertheless filled with liquid He and acted as a cryopump.

The small auxiliary chamber (No. 17) serves both as a vacuum interlock and as a sample preparation chamber. It is separately pumped and is connected to the main chamber by a straight-through uhv valve (No. 15). New crystals can be loaded into the storage wheel (No. 7) of the photoemission chamber without breaking the photoemission-chamber vacuum. They are first loaded into the movable carriage (No. 16) and the small chamber is pumped down and baked out. The valve to the photoemission chamber may then be opened and the crystals transported by a rack and pinion and placed with the cleaving gripper (No. 13) into the storage wheel. The activation of the samples can be carried out in the preparation chamber without exposing the photoemission chamber to cesium and oxygen. For the GaAs measurements, the sample preparation chamber was outfitted with Cs channels, an oxygen leak, and a provision for measuring the photocurrent of a sample during activation (not shown in Fig. 4).

The GaAs crystals studied were p-type doped

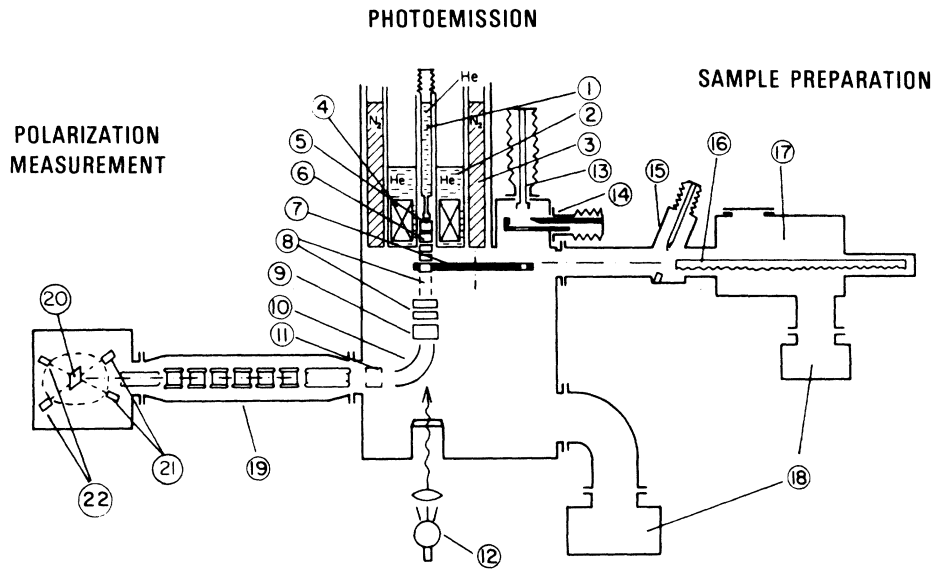

FIG. 4. Schematic diagram of the apparatus: 1, Movable He cryostat with sample gripper; 2, He cryostat; 3, liquid nitrogen; 4, superconducting coil; 5, sample in measuring position; 6, accelerating electrodes; 7, rotatable wheel with samples; 8, parallel beam shifters; 9, plane condenser; 10, cylindrical condenser; 11, aperture; 12, light source; 13, gripper for cleaving; 14, cleaving mechanism; 15, ultrahigh-vacuum valve; 16, rack-and-pinion linear motion; 17, sample preparation chamber; 18, ion-getter pumps; 19, seven-stage accelerator; 20, gold foil; 21, detectors to measure Mott asymmetry; 22, forward detectors to monitor beam.

with 1.3×10^{19} cm^{-3} Zn. They were purchased[30] as $5\times5\times10$-mm^3 single crystals which we cut into $2.5\times2.5\times5$-mm^3 pieces such that one of the faces was the (110) cleavage plane. The crystals were fastened either mechanically or with silver paint into holders suitable for the grippers (No. 1 and 13).

The activation of the GaAs surface proceeds as follows. A crystal is cleaved between the blade and the anvil (No. 14). It is then immediately lowered into the movable carriage and transported to the sample preparation chamber for activation. There Cs is evaporated from a Cs-metal dispenser[31] for such a time that the photocurrent produced by the light of a 2-W incandescent lamp reaches a maximum. Oxygen[32] is then admitted at a pressure of 2×10^{-8} Torr until the photocurrent decreases to about half its value. Subsequent cesiation brings the photocurrent to a new maximum. Depending on the desired number of layers, these procedures are repeated. A typical oxygen exposure was 0.6 langmuir (1 L = 10^{-6} Torr sec). The gas composition in the preparation chamber could be analyzed and recorded with a Vacuum Generators quadrupole mass spectrometer. The base pressure in the preparation chamber was 6×10^{-9} Torr. After finishing the surface treatment, the crystal is moved back into the main chamber where the sample gripper lifts it to the measuring position. The base pressure during measurement was 3×10^{-10} Torr.

Circularly polarized light was produced in a standard way. The light from a mercury-xenon arc lamp (Hanovia 901B-1) was monochromatized using a Zeiss M4QIII monochromator. Subsequently it passed through a polaroid linear polarizer and a variable retarder of the Soleil-Babinet type to produce the circular polarization.

The measured spin polarization can be corrected for the imperfect circular polarization of the light in the following way. Generally, the light transmitted by the retarder is not completely circularly polarized but is elliptically polarized. Elliptically polarized light can be decomposed into σ^+ and σ^- circularly polarized light of intensity I_+ and I_-. The circular polarization is defined as $P_{cp}=(I_+-I_-)/(I_++I_-)$. We did not measure I_+ and I_- directly, but measured the light transmitted by a linear polarizer located behind the retarder. When the linear polarizer is rotated by 2π, the intensity goes through maxima I_{max} and minima I_{min}. One finds for the degree of circular polarization $P_{cp}=2(I_{min}I_{max})^{1/2}/(I_{min}+I_{max})$. The variability of the Soleil-Babinet retarder enabled us to maintain $P_{cp}>99\%$. The previously published values of spin polarization (Refs. 2 and 3) were 10% too high owing to an improper correction for the degree of circular polarization of the light.

IV. RESULTS AND DISCUSSION

The spectra of spin polarization $P(\hbar\omega)$ were measured on seven different samples. Some measurements of $P(\hbar\omega)$ were made as a function of temper-

ature and as a function of Cs and O coverage. In addition the yield was measured at least once for each sample.

A. Photoelectric yield

The yield of electrons per incident photon is useful in characterizing the prepared sample surface. A typical yield from one of our treated GaAs samples is shown as curve (a) in Fig. 5 compared to the yield of an optimized photocathode[33] shown as curve (b). Curve (a) was measured at $T \leq 10$ K and its threshold is therefore 0.1 eV higher than that of curve (b), which was measured at room temperature. The yield from our sample increased more slowly at threshold and remained lower in magnitude than that of an optimally treated GaAs surface. This can be traced to the marginal vacuum (6×10^{-9} Torr) in the preparation chamber and perhaps to contamination from the Cs channels. Similar effects have been observed by Baer[34] on samples intentionally aged before Cs and O treatment. The yield curves show that at least a zero electron affinity was obtained on our samples in all but two cases where we believe the electron affinity was slightly positive. Except for these two cases, which exhibit some interesting features discussed in detail below, we do not believe that the fact that our samples were not optimal photocathodes significantly influences the spectra of spin polarization.

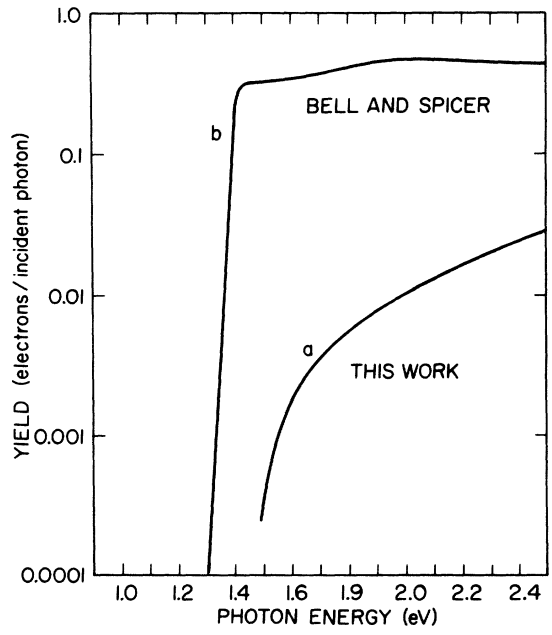

FIG. 5. Photoelectric yield (a) of GaAs + Cs(OCs)[1] measured at $T \leq 10$ K, and (b) of an optimized photocathode measured at room temperature (Ref. 33). The high yield (b) of an optimized photocathode makes GaAs the best known photoemitter.

B. Spectrum near threshold

The spectrum $P(\hbar\omega)$ measured on a sample at temperature $T \leq 10$ K is shown in Fig. 6. The rectangular fields represent the uncertainty in the measured points. The polarization has a maximum of 40% at threshold, in agreement with luminescence measurements of Ekimov and Safarov.[14] This agreement is not unexpected, because for a negative-electron-affinity photoemitter the photoemission time τ_{pe} is governed by the electron recombination time τ_e, that is, $\tau_{pe} \approx \tau_e$. The polarization is less than the theoretical value of 50% if the spin flips before the electron is emitted, a process characterized by the emission time τ_{pe} and the spin relaxation time τ_s according to Eq. (9). Spin exchange scattering is also possible in the Cs-O layer. In preliminary tests of the effect of thicker Cs-O layers, the maximum P in the case of GaAs + Cs(OCs)[5] was 33%.

For $\hbar\omega > E_g + \Delta$, the polarization decreases to zero as emission from the split-off valence band with $P = -100\%$ is mixed in. In a first approximation of parabolic bands and matrix elements independent of k, the excitation probability $w(\omega)$ for the split-off band is

$$w_i(\omega) = \int d^3k \, |M_i|^2 \delta(E_f(\vec{k}) - E_i(\vec{k}) - \hbar\omega)$$

$$\propto \sum_\sigma |M_{i\sigma}|^2 (\mu_i)^{3/2} (\hbar\omega - E_g - \Delta)^{1/2} , \qquad (11)$$

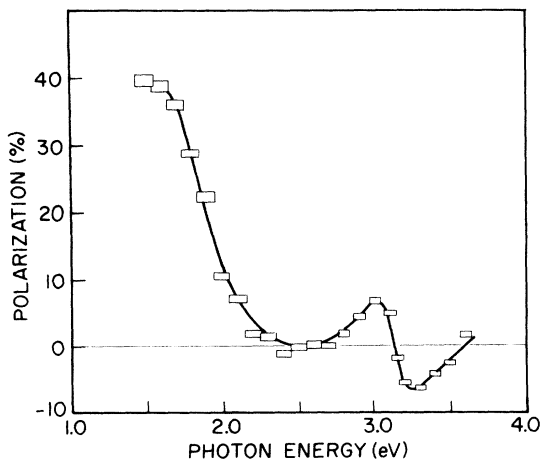

FIG. 6. Spectrum of spin polarization from GaAs + CsOCs at $T \leq 10$ K [the same sample and conditions as curve (a) of Fig. 5] . Note the high value of $P = 40\%$ at threshold ($\hbar\omega \sim 1.5$ eV) and positive and negative peaks at $\hbar\omega = 3.0$ and 3.2 eV.

and for the upper valence bands

$$w_i(\omega) \propto \sum_\sigma |M_{i\sigma}|^2 (\mu_i)^{3/2} (\hbar\omega - E_g)^{1/2} , \qquad (12)$$

where μ_i is the reduced mass between the effective mass of the conduction band and the effective mass of the ith valence band, $1/\mu_i = 1/m_c^* + 1/m_i^*$, and $M_{i\sigma}$ is the matrix element of the electromagnetic interaction coupling the ith valence band and the state of spin σ of the conduction band. The decrease of the polarization to zero is not abrupt because the onset of transitions from the split-off band varies as $(\hbar\omega - E_g - \Delta)^{1/2}$.

There is also a slight decrease in P above threshold before the onset of emission from the split-off band. An exact calculation of the variation in P as a function of $\hbar\omega$ should include the changes in wave function away from $k = 0$.[35] For the purposes of interpreting our spectra, we can use the wave functions calculated by Kane[10] in the $\vec{k} \cdot \vec{p}$ approximation. From Eq. (14) of Ref. 10 we have the wave functions of the conduction band, heavy- and light-hole bands, and split-off band, labeled 1–4, respectively;

$$\begin{aligned} \Psi_{i\alpha} &= a_i S\uparrow + b_i[(X - iY)\downarrow/\sqrt{2}\,] + c_i Z\uparrow , \\ \Psi_{i\beta} &= a_i S\downarrow + b_i[-(X + iY)\uparrow/\sqrt{2}\,] + c_i Z\downarrow , \end{aligned} \qquad (13a)$$

where i takes the value 1, 3, or 4, and for the heavy-hole band

$$\begin{aligned} \Psi_{2\alpha} &= (X + iY)\downarrow/\sqrt{2} , \\ \Psi_{2\beta} &= (X - iY)\uparrow/\sqrt{2} . \end{aligned} \qquad (13b)$$

The coefficients a_i, b_i, c_i reduce at $k = 0$ to the values given in Table I. In the region around $k = 0$ they depend on k and can be calculated using the approximations given by Kane [Eqs. (12) and (15) of Ref. 10] and the effective masses for GaAs which are [36] $m_1^*/m = 0.067$, $m_2^*/m = 0.62$, $m_3^*/m = 0.074$, and $m_4^*/m = 0.15$. Figure 7 shows the coefficients for the conduction band and the light-hole band. Note that while the heavy-hole band is independent of k as one moves away from $k = 0$, there is an increasing admixture of s wave function in the light-hole band and an increase in b_3 relative to c_3. This leads to a k-dependent decrease in the polarization over the region $E_g < \hbar\omega < E_g + \Delta$.

At first glance it seems that if we could isolate the transitions from the heavy-hole states, which from Eq. (13) correspond to the wave functions $|\frac{3}{2}, \frac{3}{2}\rangle$ and $|\frac{3}{2}, -\frac{3}{2}\rangle$ of Table I, we could achieve a polarization of 100%. Moreover, from Eq. (12) it is apparent that the transition probability from the heavy-hole band is higher than from the light-hole band owing to the larger effective mass and resulting higher density of states, which according to the foregoing argument should lead to a higher P. The fallacy in such reasoning is that the wave functions of Eqs. (13) take this simple form only along a single direction in k space. Owing to the symmetry at Γ, this single direction is arbitrary. At other symmetry points in the Brillouin zone, the wave functions take a simple form only if the direction is a symmetry axis (see Sec. IV D).

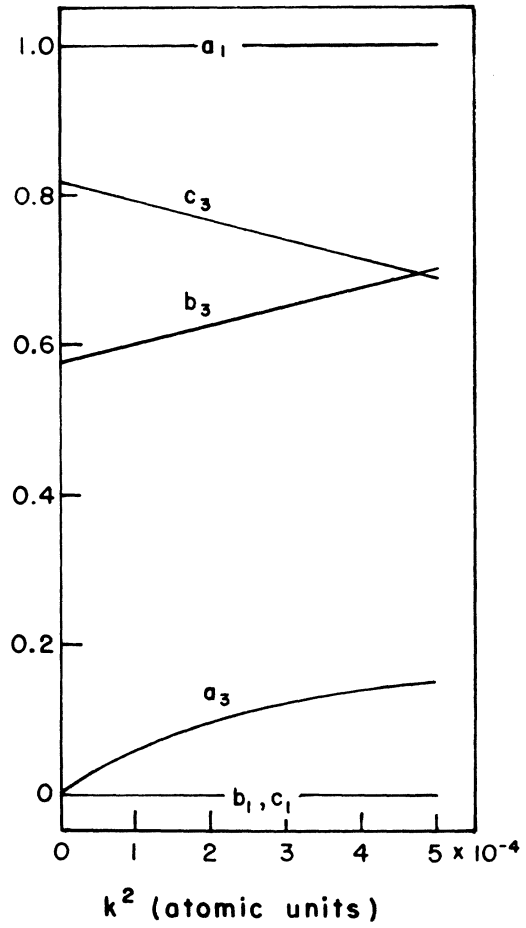

FIG. 7. Coefficients a_i, b_i, and c_i of Eq. (13a) calculated for the conduction band ($i = 1$) and the light-hole valence band ($i = 3$) for small k.

We are interested in the matrix elements $\langle \psi_f | H_{int} | \psi_i \rangle$, where H_{int} is proportional to $X \pm iY$ for $\sigma^\pm$ light in a coordinate system in which the z direction is defined by the angular momentum of the circularly polarized light. In general, the light is not incident along the direction which specifies the coordinate system in which the wave functions take a simple form. To calculate the matrix element we express the wave functions in a coordinate system defined by the angular momentum of the light by

rotating the spatial and spin parts of the wave function.

The polarization is calculated by summing the transition probabilities to states with spin parallel and antiparallel to the quantization axis over the appropriate directions in k space. The polarization resulting from the ith valence band is given in terms of the matrix element $M_{i\sigma}$ as

$$P_i = -\frac{|M_i\uparrow|^2 - |M_i\downarrow|^2}{|M_i\uparrow|^2 + |M_i\downarrow|^2}, \tag{14}$$

where the minus sign appears because we defined P in Eq. (1) in terms of the electron magnetic moments, and

$$|M_i\uparrow(\downarrow)|^2 = \int d\Omega' |\langle S\uparrow(\downarrow)|H_{\text{int}}|\Psi_{i\vec{k}}\rangle|^2 \tag{15}$$

for excitation to the final state $S\uparrow(\downarrow)$ with spin parallel $\uparrow$ (antiparallel $\downarrow$) to the angular momentum of the light. The prime in the angular integral denotes an integration over a particular region of k space. The appropriate region of k space for NEA GaAs is the whole space since even electrons initially excited into a state where they move away from the surface may finally escape because of multiple scattering. One finds $P_i = 50\%$ for i corresponding to the heavy-hole band. Thus in photoemission from NEA GaAs it is not possible to increase the polarization above 50% by limiting excitations to the heavy-hole band. This result has been discussed in connection with luminescence experiments by Fishman.[37] Calculations for luminescence show that P_i corresponding to the light-hole band and split-off band is 50% and −100%, respectively.[35,37]

C. Anomalies in the spectrum near threshold

The spectra from two of the seven surfaces studied behaved anomalously near threshold. Two new features were observed, as shown in Fig. 8. First there is the depolarization at threshold. Second, the maximum attains a value of 54%, higher than the theoretical maximum and, in addition, occurs at a higher photon energy than in Fig. 6. We suggest that this behavior is consistent with these two surfaces having a slightly *positive* rather than a negative electron affinity. While the yield curves measured for these two surfaces had a shape like curve (a) of Fig. 5, they were shifted about 0.1 eV higher in energy, supporting the idea that the electron affinity was positive for these surfaces.

The situations for positive and negative electron affinity are compared schematically in Fig. 9. In the case of a negative electron affinity, electrons in the conduction-band minimum can escape into vacuum and are, in fact, accelerated as

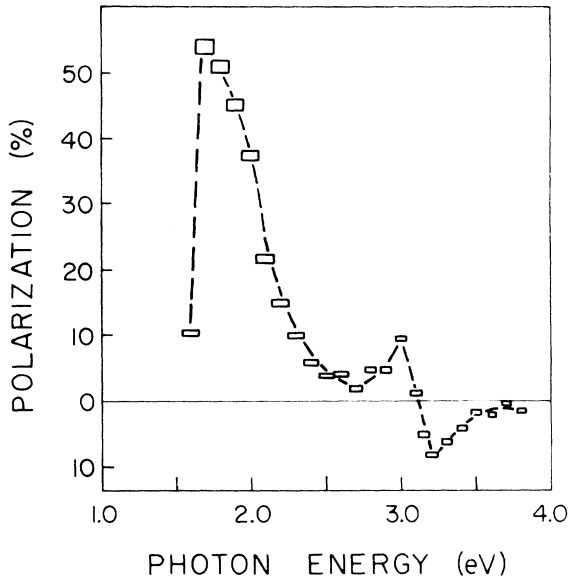

FIG. 8. Spectrum of spin polarization from GaAs + Cs-OCs measured at $T \lesssim 10$ K. This is one of two surfaces which exhibited the anomalous behavior of (1) depolarization at threshold, (2) maximum $P > 50\%$, and (3) a shift of the peak to higher photon energy. These features can be explained by a slight positive electron affinity at the surface.

they pass through the band-bending region and travel through the Cs-O layer with high velocities. In contrast, in the positive-electron-affinity (PEA) case, electrons at the conduction-band minimum cannot escape into vacuum. Higher photon energies are required so that the electrons have sufficient energy to escape over the vacuum level. At threshold, photoelectrons have nearly zero energy and travel slowly through the Cs-O layer. Such electrons have a much higher probability of scattering in the Cs-O layer. It has been experimentally demonstrated in atomic physics experiments that spin-exchange scattering from alkali atoms is very large and increases rapidly as the electron energy decreases.[38] If the Cs-O activation layer is not stoichiometric Cs_2O but has a Cs excess as suggested by Clark,[22] these cesium atoms provide the means for spin-exchange scattering of the low-energy electrons leading to the depolarization observed in Fig. 8. The depolarization at threshold and the fact the photon energies greater than E_g are required for emission in the PEA case also explain the shift in the maximum of the polarization to higher energy.

The maximum value of $P = 54\%$ is a consequence of the PEA restricting the emission directions to a cone of half-angle θ_c about the normal to the surface. In a quasiclassical picture, an electron

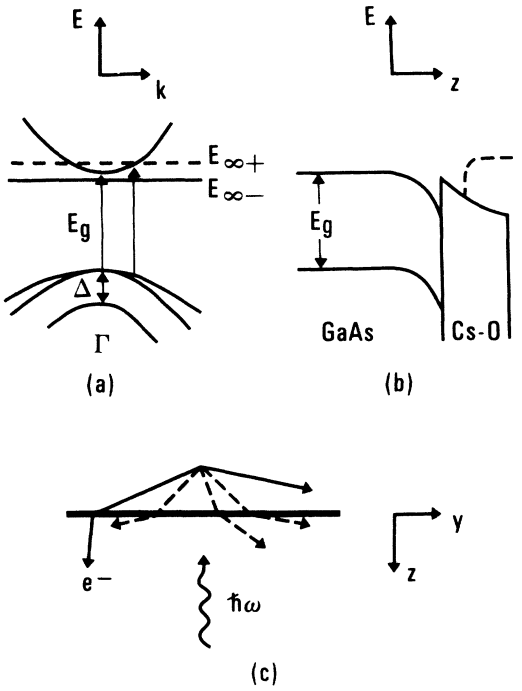

FIG. 9. Photoemission from positive- and negative-electron-affinity GaAs compared in three different spaces: (a) E vs k, (b) E vs z, and (c) z vs y. The dashed line corresponding to the positive-electron-affinity case represents the vacuum level $E_{\infty+}$ in (a), and the surface barrier in (b); these result in the electron emission being confined to an escape cone in the material (c) and the electrons losing energy at the surface. In contrast, in the NEA case the electron emission is not confined to a cone in the material and the electrons gain energy on emission.

which escapes must have momentum $p_z = p\cos\theta$ normal to the surface such that $p_z^2/2m > \chi$. Consequently, the escape cone half-angle $\theta_c = \cos^{-1}[(2m\chi/p^2)^{1/2}]$. For isotropic excitation, the escape probability $T(E)$ is just the fraction of electrons in the cone of electrons having sufficient energy to overcome the surface barrier,

$$T(E) \equiv \frac{1}{4\pi}\int_0^{\cos^{-1}\theta_c}\int_0^{2\pi} d\Omega = \frac{1}{2}\left[1-\left(\frac{\chi}{\chi+E}\right)^{1/2}\right], \tag{16}$$

where E is the kinetic energy of the electron with respect to the vacuum level. [This approximation for $T(E)$ ignores quantum-mechanical reflection at the surface barrier[39] or trapping in surface states,[40] which even for NEA GaAs reduces the escape probability of the threshold electrons to about 30%.] In the parabolic-band approximation, which we have been using near $k=0$, the kinetic energy is related to $\hbar\omega$ as $E = (\mu_i/m_1^*)(\hbar\omega - E_g)$ $-\chi$, so we can as well write $T_i(\omega)$. The angular integral of Eq. (15) is restricted to the limited solid angle into which emission occurs. The polarization from the heavy-hole band is therefore no longer 50% but lies between 50% and the limiting case of 100% for emission only along the quantization axis.[41]

In calculating the polarization, since P_i from the light- and heavy-hole bands are no longer the same, we must take into account the difference in the transition probabilities from the heavy- and light-hole bands [$w_2(\omega)$ and $w_3(\omega)$], and the difference in the escape functions [$T_2(\omega)$ and $T_3(\omega)$] for electrons excited from the two bands with a given $\hbar\omega$. In adding the polarization P_i from each band to obtain the total polarization P we have

$$PI = \sum P_i I_i \ , \tag{17}$$

where the photocurrent from the ith valence band $I_i \propto w_i(\omega)T_i(\omega)$ and the total current $I = \sum I_i$. For $\hbar\omega < E_g + \Delta$, where we have emission only from the heavy- and light-hole bands ($i = 2$ and 3), the spin polarization is

$$P(\omega) = \frac{P_2(\omega)T_2(\omega)w_2(\omega) + P_3(\omega)T_3(\omega)w_3(\omega)}{T_2(\omega)w_2(\omega) + T_3(\omega)w_3(\omega)} \ . \tag{18}$$

We consider an example to illustrate how a polarization greater than 50% is obtained. For $\hbar\omega = E_g + 0.15$ eV, electrons excited from the heavy- and light-hole bands have energies $\chi + E$ with respect to the conduction-band minimum of 135 and 78 meV, respectively. If we take χ to be 68 meV, for example, then $T_2 = 0.146$ and $T_3 = 0.035$, and the corresponding escape cone half-angles are 45° and 21°, respectively. Performing the integral of Eq. (15) for the heavy-hole band over the region bounded by $\theta_c = 45°$ and using Eq. (14) we find $P_2 = 86\%$. For the purpose of this illustration, we approximate the integral over the small solid angle required for P_3 by the quantization-axis value of −100%; this will lead to a somewhat lower total polarization. The ratio of the transition probabilities $T_2(\omega)/T_3(\omega)$ depends on $(\mu_2/\mu_3)^{3/2} = 2.25$ and the ratio of the square of the matrix elements, which is 3 at $k=0$. However, for $\hbar\omega = E_g + 0.15$ eV, transitions from the light-hole band occur at $k^2 = 3.9\times10^{-4}$ a.u. and from Fig. 7 this gives $b_3 = 0.075$; so the ratio of the square of the matrix elements is 2.19. The polarization from Eq. (18) is then 77%. In this way, it is possible to obtain a polarization larger than 50%. The value $P = 77\%$ of this example indicates that χ was likely less than 68 meV to give the experimental value $P = 54\%$; however, χ cannot be accurately determined in this way in the absence of a quantitative knowledge of the spin-exchange scattering.

D. Transitions at $L(\Lambda)$

The spectra of Figs. 6 and 8 both exhibit a positive and negative peak at 3.0 and 3.2 eV, respectively, which can be understood in terms of transitions of [111] symmetry. The relevant part of the energy-band diagram from Zucca *et al.*[42] is shown in Fig. 10. In going from Γ to L, the valence band at Γ_7 connects to L_6 (not shown), which is split off by the crystal field. At L, the upper valence band (L_3 in nonrelativistic notation) is split by the spin-orbit interaction into the doubly degenerate state at L_6 and degenerate L_4 and L_5 states. The conduction and valence bands are parallel along the Λ symmetry axis from about $(2\pi/\alpha)(0.2, 0.2, 0.2)$ to $(2\pi/\alpha)(0.5, 0.5, 0.5)$,the L point.[8] Even though the arrows in Fig. 10 indicating transitions have been drawn near L, contributions are expected all along the parallel band region of the [111] axis. The structure in our spectra is due to transitions from L_4 (Λ_4) and L_5 (Λ_5) to L_6 (Λ_6), labeled C in Fig. 10, which occur with equal probability but go to the opposite spin state from transitions L_6 (Λ_6) to L_6 (Λ_6), labeled D in Fig. 10. The positions of the extrema at 3.0 and 3.2 eV agree well with the band separations of 3.04 and 3.26 eV determined by Schottky barrier electroreflectance measurements.[8]

The structure arising from transitions along Λ has a different shape from the structure we have discussed which is due to transitions at Γ. This is because, even though the bands bend away from each other as one moves perpendicular to the [111] axis, there is a larger region in k space than at Γ in which the energy surfaces are approximately parallel. Thus, as the photon energy is increased, the transitions labeled C are first observed, giving the positive peak, and then the transitions labeled D dominate, giving rise to the negative peak. In contrast, at Γ transitions labeled A from the upper valence band continue to be competitive as transitions labeled B from the split-off band begin.

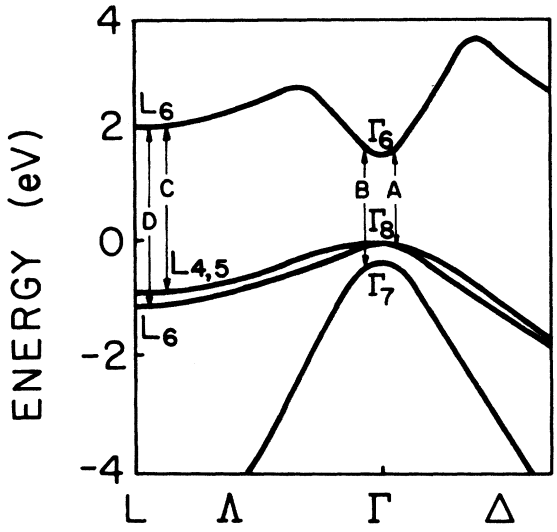

FIG. 10. Energy-band diagram of GaAs showing the transitions at Γ and L which give rise to the structure in our measured spectra (after Ref. 42).

For a better understanding of the structure due to transitions along Λ, we investigate the wave functions of the states of interest. The angular and spin part of the wave functions as given by Pollak and Cardona[43] are listed in Table II. We need consider only the s states of the conduction band to which transitions from the p valence states are allowed. For σ^+ polarized light in the [111] direction, for example, we would have transitions from $L_{4,5}$ with wave function $|(X-iY)\downarrow\rangle/\sqrt{2}$ to $|S\downarrow\rangle$ and from L_6 with wave function $|(X-iY)\uparrow\rangle/\sqrt{2}$ to $|S\uparrow\rangle$ which would give 100 and -100% polarization, respectively, if it were possible to isolate the excitation to states on the quantization axis.

With the quantization axis in the [111] direction, the [111] and $[\bar{1}\bar{1}\bar{1}]$ directions are no longer equivalent to the other six directions $[11\bar{1}]$, $[\bar{1}\bar{1}1]$, $[\bar{1}11]$, $[1\bar{1}\bar{1}]$, $[1\bar{1}1]$, and $[\bar{1}1\bar{1}]$. To find the contribution from states not on the quantization axis we rotate a wave function expressed in a coordinate system along the $[11\bar{1}]$ direction, for example, and express it in terms of the spatial and spin coordinates of the reference system, where the z direction is defined by the angular momentum of the light and the dipole transition operator takes the form $X \pm iY$. The transition probabilities $|M_i\uparrow(\downarrow)|^2$ to conduction-band states with spin parallel (antiparallel) to the light angular momentum are then calculated as at Γ. For purposes of illustration, we will calculate P at the L point and not be concerned with the angular integration over wave functions for a general $\vec{k}$ direction in the

TABLE II. Angular and spin part of the wave functions at L (Λ).

Symmetry point	Wave function
L_6 (Λ_6)	$A\|S\uparrow\rangle + B\|Z\uparrow\rangle$
	$A\|S\downarrow\rangle + B\|Z\downarrow\rangle$
L_4, L_5 ($\Lambda_{4,5}$)	$(\frac{1}{2})^{1/2}\|(X+iY)\uparrow\rangle$
	$(\frac{1}{2})^{1/2}\|(X-iY)\downarrow\rangle$
L_6 (Λ_6)	$(\frac{1}{2})^{1/2}\|(X+iY)\downarrow\rangle$
	$(\frac{1}{2})^{1/2}\|(X-iY)\uparrow\rangle$

neighborhood of L. If it were possible to isolate the transitions from states along the six axes of [111] symmetry which do not coincide with the light angular momentum, one would find $P = 20\%$. The initial polarization in the solid is calculated by taking the transitions at all eight critical points together. In this case, Eq. (15) is written

$$|M_i\uparrow(\downarrow)|^2 = \sum_L |\langle S\uparrow(\downarrow)|H_{\rm int}|\Psi_{iL}\rangle|^2 . \quad (19)$$

The $|M_i\uparrow(\downarrow)|^2$ are used in Eq. (14) to obtain $P_L = 50\%$.

Unlike the situation at Γ, the distribution of excited states at L is anisotropic and emission occurs preferentially along certain directions. Not all of the eight symmetry directions included in Eq. (19) contribute to the direct emission. Which electrons are emitted depends on the crystal surface orientation, and their polarization depends on the angular momentum of the light with respect to the [111] symmetry direction. Additionally, the polarization at photon energies corresponding to transitions to the L minima has contributions not only from the direct emission but also from electrons which have been scattered. Some of the electrons excited to an L minimum of the conduction band may scatter to the Γ minimum, where they will contribute to the isotropic distribution of thermalized electrons. On the other hand, electrons excited near Γ to states higher than the L or X minima have a substantial probability of scattering into these higher-lying minima.[40]

We first calculate the polarization of the direct emission at L. We consider excitation across the gap from an initial state at wave vector $\vec{k}$ to a final state at $\vec{K} = \vec{k} + \vec{G}$. For transitions from an initial state at the L point $(\pi/a)(\bar{1},\bar{1},\bar{1})$, for example, only $\vec{G} = (2\pi/a)(1,1,1)$ along the same axis can conserve both energy and momentum, and emission is along this $\vec{G}$ direction. Not all of the eight [111] directions along which electrons are excited allow emission into the vacuum. The component of $\vec{K}$ parallel to the surface, $K_\parallel$ is conserved on emission. For emission of an electron into vacuum we must have

$$E_L - E_\infty > \hbar^2 K_\parallel^2/2m , \quad (20)$$

where E_L and E_∞ are the energies of the L minimum and the vacuum level, respectively.[21] For a (110) crystal surface, as in our experiment, only transitions from initial states $\vec{K} - \vec{G}$ with $\vec{G}_{111}$ and $\vec{G}_{11\bar{1}}$ give rise to direct emission according to Eq. (20). In our experimental configuration, where the angular momentum of the light is along the [110] direction, the polarization expected as a result of emission along $\vec{G}_{111}$ and $\vec{G}_{11\bar{1}}$ is $P \sim 35\%$.

It is not surprising that the experimental value $P = 8\%$ is lower than the calculated value when account is taken of the other contributions to the photocurrent. Electrons excited to energies higher than the L minimum, e.g., at Λ, can undergo intervalley scattering via optical phonons and scatter from one state of [111] symmetry to another.[40] For example, *unpolarized* electrons excited from initial states $\vec{K} - \vec{G}$, with $\vec{G}_{1\bar{1}\bar{1}}$, $\vec{G}_{\bar{1}11}$, $\vec{G}_{\bar{1}\bar{1}1}$, and $\vec{G}_{\bar{1}\bar{1}\bar{1}}$ which lie in the surface, can contribute to the emission from the L valleys along [111] and [11$\bar{1}$]. Moreover, electrons excited not far from Γ, and which have $P \sim 0$ at $\hbar\omega \sim 3$ eV, can scatter into an L minima and thereby decrease P. The polarization may also be reduced owing to transitions at the same $\hbar\omega$ at some general point in the Brillouin zone where the polarization is small. Finally, the possibility of spin-flip scattering before emission could further reduce P.

E. Outlook

The results obtained from this initial series of measurements suggest a number of promising areas for further investigation. Because no magnetic field is required, it is straightforward to analyze the kinetic energy of the electrons in addition to their spin, that is to measure $P(\hbar\omega, E)$ instead of $P(\hbar\omega)$ as we have done so far. While it is in principle possible to measure the energy distribution of the photoelectrons with a magnetic field present, the very low brightness of the photoemitter in the presence of a magnetic field and the unavailability of an efficient detector has prevented such measurements.

A measurement of $P(\hbar\omega, E)$ enables one to determine separately the polarization of electrons thermalized to L or X minima as distinct from those at the Γ minimum. Because the spin polarization of the electrons in effect "tags" the electrons with respect to their point of origin, intervalley scattering can be studied.

The electron recombination time τ_e and the spin relaxation time τ_s can be determined independently for excitations just across the forbidden gap using luminescence measurements. Spin-polarized photoemission offers a method to study the spin relaxation time as a function of electron kinetic energy. Both the spin and electron relaxation times are expected to depend on the kinetic energy. The hot-electron lifetime is expected to be relatively temperature independent, allowing the temperature dependence of τ_s to be determined for various electron energies.

Definitive measurements of $P(\hbar\omega)$ as a function of temperature are of great interest and have not yet been carried out. The spectra of Figs. 6 and 8 were observed at $T \leq 10$ K. For an emitter exhibiting the characteristics of a PEA, a spectrum very similar to Fig. 8 with a maximum $P = 54\%$ was

recorded at $T \approx 80$ K, whereas otherwise the maximum P at this temperature was 32%. Polarizations as high as 25% were observed at room temperature. The temperature dependence of the polarization arises from the strong temperature dependence of τ_s relative to τ_{pe} in Eq. (9). τ_{pe} is shorter for a PEA surface than for an NEA surface, giving rise to a higher P at a given temperature for these surfaces.

We of course want to check that the polarization of electrons emitted from an optimally activated photocathode remains high. An investigation of the mechanism of the depolarization which was observed for positive-electron-affinity surfaces is also important. Measurements in which the thickness of the activation layer is varied and the Cs excess in Cs-rich Cs_2O is controlled can clarify the role of spin-exchange scattering from atomic Cs when Cs is used to lower the vacuum level of materials.

Because the band structure of GaAs is well known, GaAs is an ideal material for demonstrating the sensitivity of spin-polarized photoemission to the spin-dependent aspects of electronic structure. A negative electron affinity is not required; all that is necessary is that the final state of interest lie above the vacuum level. The technique is not limited to GaAs nor even to semiconductors. Heinzmann *et al.* have measured the spin polarization of photoelectrons from alkali-metal films.[44] Koyama and Merz have discussed the application of measurements of $P(\hbar\omega, E)$ to determine the spin-dependent electronic structure of metals.[45] We expect that the most interesting applications of spin-polarized photoemission to probe spin-dependent electronic structure will be realized in materals where less is known about the electronic structure than in our test case, GaAs.

V. NEA GaAs AS A SOURCE OF POLARIZED ELECTRONS

A good source of spin-polarized electrons has been sought for many years for experiments in high-energy physics[46] and atomic physics.[47] Having a source with the qualities of the GaAs source, several intriguing experiments with solids can also be considered.

In order to assess NEA GaAs as a source of spin-polarized electrons, we review briefly the criteria for a good source. Both high current and high polarization are desirable. When the experimental uncertainty is limited by the counting statistics, a figure of merit for a source of polarized electrons is P^2I. For most experiments it is necessary to reverse the polarization to eliminate systematic effects such as apparatus asymmetries. Being able to reverse the polarization without otherwise affecting the electron beam characteristics is an important advantage, as is the capability to rapidly modulate the polarization. The energy spread ΔE of the electrons may also be important.

Since a source is coupled with an electron optical system to form and transport the beam, an important characteristic of the source is its brightness or Richtstrahlwert, defined as[48]

$$R = \frac{dI}{dA\,d\Omega} , \tag{21}$$

where dI is the current through a differential area dA and $d\Omega$ is the solid angle subtended by the electrons. As pointed out by Kuyatt and Simpson,[48] along a beam path where the current is conserved and there are no energy dispersing devices, R/E, where E is the electron energy, is a conserved quantity and a measure of the electron optical quality of the source. A frequently specified quantity is the emittance, defined as $\epsilon = \rho\alpha$, where ρ is the radius of the electron beam at the source and α is the aperture angle. The brightness R is proportional to I/ϵ^2, and since R/E is the conserved quantity, the emittance is specified at a given energy.

For electrons produced in axially symmetric electric and magnetic fields the effective emittance can be shown to be[49]

$$\epsilon = \rho_0 (E_0/E)^{1/2} + \tfrac{1}{2}(e/m)\,\rho_0^2 B_0/v , \tag{22}$$

where ρ_0 is the maximum initial distance from the axis, E_0 and E are the initial and final kinetic energies, B_0 is the magnetic field at the electron source, and v is the final velocity of the electron. The second term in Eq. (22), which is nonzero only when a magnetic field is present, derives from the fact that the axial component of the canonical angular momentum $\vec{L} = \vec{v} \times (m\vec{v} + e\vec{A})$ is conserved; electrons produced off axis will have skewed trajectories in a region of zero magnetic field. Therefore, sources which employ a magnetic field generally have lower brightness than similar sources without a magnetic field (a possible exception is the field emission source because ρ_0 is extremely small).

Consider now the properties of NEA GaAs with respect to the criteria for a good source of polarized electrons discussed above. The current which can be obtained is the product of the yield from Fig. 5 and the number of incident photons per sec. For the measurements reported here, where we made no attempt to optimize the source, a current of the order of 1 μA was obtained. Note that a current of 1 mA can be obtained from the photocathode having yield (b) of Fig. 5 with a light power of 5 mW. As with thermal cathodes, the resulting electron beam may be space charge limited for

some beam energies. The photothreshold energy of GaAs is in the range of intense dye-laser light sources. The photothreshold can be increased a few tenths of an eV to match a particular light source while maintaining the polarization by using a direct-gap ternary compound such as GaAlAs or GaAsP.

A polarization in the neighborhood of 50% is substantial. Note that applying the figure of merit P^2I this is equivalent to a 100% polarized source with $\frac{1}{4}$ the current.[50] An attractive feature of the GaAs source is the easy and rapid reversal of the spin polarization by simply reversing the sense of the circular polarization of the light, which does not affect electron optics. In contrast, in systems employing a magnetic field to specify the preferred direction, less rapid reversal of the polarization is possible and is difficult to achieve without slight changes in the electron optics. With the GaAs source, the polarization of the electron beam can be modulated and lock-in techniques used to detect even small spin-dependent effects in an interaction.

NEA GaAs is a very bright source of polarized electrons. The light incident on the photocathode can easily be focused to give a source area less than 1 mm in diameter. The emission from a NEA surface is very directional owing the small internal effective mass of the electrons and the NEA, which causes an acceleration of the electrons on emission.[21] Pollard[51] has reported that near threshold electrons are emitted into a cone of 5° half-angle with a subtended solid angle of 7.6 $\times 10^{-3}$ sr. Because the source is operated near photothreshold in the region of high polarization, the initial beam energy and energy spread are only 0.1–0.2 eV. From these data we calculate an emittance of 2 mrad cm at 1 eV.

Table III lists some competitive sources. A comparison of sources of polarized electrons is very difficult because only a few processes which produce polarized electrons have been optimized as sources, and then often for special, noncomparable purposes. Other lists of sources available up to 1972 can be found in Refs. 49 and 52. The values in square brackets in the table are projected values which, in our opinion, have a high probability of being achieved.

A few comments on the eight sources listed in the table are warranted. The photoionization of Li has been optimized[53] as a pulsed source with the given emittance appropriate for injection into the linear accelerator at the Stanford Linear Accelerator Center (SLAC). Measurements of the polarization after electron acceleration to 19.4 GeV have been recently reported.[54] The relatively high polarization is advantageous in situations where polarization cannot be traded for higher

TABLE III. Comparison of some sources of spin-polarized electrons.

Method	Ref.	$\lvert P\rvert$	Reversal of $\vec{P}$	I_{dc} (A)	I_{pulse}	E (eV)	ΔE (eV)	H (kOe)	Emittance	Brightness
1. Photoemission from NEA GaAs	3	0.40	$\Delta\vec{L}$	10^{-6} [10^{-3}]	[10^{12} electrons/1.5 μsec]	0.2	0.2	0	2 mrad-cm at 1 eV	very high
2. Photoemission from EuO	27	0.61 [0.80]	$\Delta\vec{H}$	10^{-6}	3×10^{9} electrons/1.5 μsec	2	2	21 [30]		medium
3. Photoionization of polarized Li atomic beam	53	0.76	$\Delta\vec{H}$		3×10^{9} electrons/1.5 μsec		1500	0.2	7 mrad-cm at 70 keV	medium
4. Fano effect, photoionization of Cs atoms	55	0.90	$\Delta\vec{L}$		3×10^{9} electrons/0.5 μsec		500	0	0.6 mrad-cm at 115 keV	high
5. Optically pumped He discharge	56	0.30	$\Delta\vec{L}$	10^{-6}		500 [30]	0.5	0	10 mrad-cm at 500 eV	high
6. Field emission (EuS)	57	0.89	$\Delta\vec{H}$	[10^{-6}]			0.1	2–20		very high
7. Electron scattering from Hg atomic beam	58	0.27	$\Delta\theta$	2×10^{-8}		7	0.2	0		medium
8. Electron scattering from W	62	0.40	$\Delta\theta,\Delta E$	5×10^{-8} [10^{-4}]		80	0.2	0		high

current owing target damage. Photoemission from EuO,[27] which was studied in a research apparatus not optimized as a source, appeared attractive as an alternative for SLAC but is far surpassed by NEA GaAs, both in brightness and ease of polarization reversal. The polarization is also easily reversed in sources[55,56] based on the Fano effect and on the optically pumped He discharge, which both benefit from the absence of a magnetic field. The chief drawback of the Fano-effect source is the low current obtained from the photoionization of the atomic beam. The parameters reported for source 5 are for an optimized optically pumped He discharge source. Because of the small emitting area, the field-emission source[57] is very bright in spite of the presence of a magnetic field of 2 kOe. The current is limited by the strength of the electric field that can be applied without too rapid deterioration of the emitting tip. The last two sources listed in Table III depend on the spin polarization produced by the spin-orbit interaction in electron scattering. The scattering of electrons at energies up to about 1 keV from an atomic beam has proven useful as a source primarily in experiments which already involved atomic beams.[58,59] While perhaps convenient in some situations, the parameters indicate that such a source is not comparable with several of the above. It should be pointed out, however, that some differential pumping is required to use an inherently ultrahigh-vacuum photoemission or field-emission source with the lower vacuums of atomic scattering experiments. The production of polarized electrons by scattering from solids was first shown by Davisson and Germer[60] in 1929 (contrary to their own conclusion[61]) and has been used to produce polarized electrons with energies from ~100 eV to ~100 keV. The most recent measurements[62] of low-energy scattering were from a W single crystal (8 in Table III). While not yet explored as a source, it appears promising. The difficulty in reversing the polarization may be overcome by varying the electron energy (P changes rapidly with energy).

From our discussion of the best existing polarized-electron sources, we see the NEA GaAs combines simplicity with high efficiency. The applications of such a source are numerous. In high-energy physics, one of the most exciting experiments will be the search for parity violations in deep inelastic electron scattering. This involves scattering of high-energy polarized electrons by unpolarized protons in a liquid-hydrogen target. A pulsed GaAs source is being built to inject spin-polarized electrons into the linear accelerator at SLAC.[63] The advent of the GaAs source makes possible electron scattering experiments from atoms and molecules which previously could only be contemplated or were the subject of a few long, laborious pioneering studies. Whereas differential cross-section measurements give $|f(\theta)|^2 + |g(\theta)|^2$, it is now relatively easy to measure the direct $f(\theta)$ and exchange $g(\theta)$ amplitudes independently, providing a more stringent test of current theories. In studies to date, polarized electrons have usually been obtained by an initial scattering experiment (7, Table III) which is surpassed by the GaAs source by at least a factor of 10^3. The high intensity and brightness of the GaAs source will permit the investigation of polarization phenomena at scattering resonances in elastic scattering and allow the study of the polarization phenomena associated with inelastic channels.[64]

In solid-state physics, spin-dependent electron scattering will be a useful new surface probe. There are two types of spin-dependent scattering experiments: first, those where the spin dependence derives from the spin-orbit interaction on scattering; this effect is found in all materials and is more pronounced for those of higher atomic number. Second, there is magnetic scattering in which the polarized beam interacts with a magnetically ordered solid through the exchange interaction; with elastic magnetic scattering surface magnetic order and surface critical phenomena can be probed.

ACKNOWLEDGMENTS

The authors are grateful to Professor H. C. Siegmann for valuable discussions throughout this work and to P. Zürcher for assistance with the initial measurements. We have benefitted from enthusiastic discussion with a number of colleagues at many laboratories. One of us (D.T.P.) is especially grateful to J. F. Herbst, J. W. Gadzuk, and D. R. Penn of NBS for helpful discussions. The financial support of the Schweizerische Nationalfonds is greatly appreciated.

---

*Present address: Surface and Electron Physics Section, National Bureau of Standards, Washington, D. C. 20234.

[1]H. C. Siegmann, Phys. Rep. C 17, 39 (1975), and references therein.

[2]D. T. Pierce, F. Meier, and P. Zürcher, Phys. Lett. A 51, 465 (1975).

[3]D. T. Pierce, F. Meier, and P. Zürcher, Appl. Phys. Lett. 26, 670 (1975).

[4]E. Garwin, D. T. Pierce, and H. C. Siegmann, Helv. Phys. Acta 47, 343 (1974). A similar proposal has

been made by G. Lampel and C. Weisbuch, Solid State Commun. 16, 877 (1975).
[5]See, for example, P. S. Farago, Adv. Electron. Electron Phys. 21, 1 (1975).
[6]C. Cohen-Tannoudji and A. Kostler, in *Progress in Optics*, edited by E. Wolf (North-Holland, Amsterdam, 1966), Vol. 5, p. 33.
[7]G. Dresselhaus, Phys. Rev. 100, 580 (1955); R. H. Parmenter, Phys. Rev. 100, 573 (1955).
[8]D. E. Aspnes and A. A. Studna, Phys. Rev. B 7, 4605 (1973).
[9]We intentionally avoid the use of "right" and "left" circular polarization, which have opposite definitions in optics and elementary particle physics. See, for example, the discussion of E. Hecht and A. Zajac, *Optics* (Addison-Wesley, Reading, Mass., 1974), Chap. 8, p. 224.
[10]E. O. Kane, J. Phys. Chem. Solids 1, 249 (1957).
[11]G. Lampel, Phys. Rev. Lett. 20, 491 (1968).
[12]R. R. Parsons, Phys. Rev. Lett. 20, 1152 (1969); Can. J. Phys. 49, 1850 (1971).
[13]A. I. Ekimov and V. I. Safarov, JETP Lett. 12, 198 (1970).
[14]A. I. Ekimov and V. I. Safarov, JETP Lett. 13, 495 (1971).
[15]D. Z. Garbuzov, A. I. Ekimov, and V. I. Safarov, JETP Lett. 13, 24 (1971).
[16]B. I. Zakharchenya, V. G. Fleisher, R. I. Dzhioev, Yu. P. Veshchunov, and I. B. Rusanov, JETP Lett. 13, 137 (1971).
[17]V. G. Fleisher, R. I. Dzhioev, B. P. Zakharchenya, and L. M. Kanskaya, JETP Lett. 13, 299 (1971).
[18]R. I. Dzhioev, B. P. Zakharchenya, and V. G. Fleisher, JETP Lett. 14, 381 (1971).
[19]G. Lampel, *Proceedings of the XII International Conference on the Physics of Semiconductors, Stuttgart, Germany, 1974*, edited by M. H. Pilkuhn (Teubner, Stuttgart, Germany, 1975).
[20]J. J. Scheer and J. van Laar, Solid State Commun. 3, 189 (1965).
[21]R. L. Bell, *Negative Electron Affinity Devices* (Clarendon, Oxford, England, 1973).
[22]M. G. Clark, J. Phys. D 8, 535 (1975).
[23]B. Goldstein, Surf. Sci. 47, 143 (1975).
[24]J. J. Uebbing and L. W. James, J. Appl. Phys. 41, 4505 (1970).
[25]G. Busch, M. Campagna, D. T. Pierce, and H. C. Siegmann, Phys. Rev. Lett. 28, 611 (1972).
[26]H. Alder, M. Campagna, and H. C. Siegmann, Phys. Rev. B 8, 2075 (1973).
[27]E. Garwin, F. Meier, D. T. Pierce, K. Sattler, and H. C. Siegmann, Nucl. Instrum. Methods 120, 483 (1974).
[28]M. Campagna, D. T. Pierce, K. Sattler, and H. C. Siegmann, J. Phys. (Paris) 34, C6-87 (1973).
[29]G. Busch, M. Campagna, and H. C. Siegmann, J. Appl. Phys. 41, 1044 (1970).
[30]Laser Diode Laboratories, Inc., Metuchen, N. J.
[31]SAES Getters, Inc., Milan, Italy.
[32]99.997%-pure research grade from Airco Industrial Gases, Riverton, N. J.
[33]R. L. Bell and W. E. Spicer, Proc. IEEE 58, 1788 (1970).
[34]A. D. Baer, Ph.D. dissertation (Stanford University, 1971) (unpublished).
[35]M. I. D'yakonov and V. I. Perel, Sov. Phys.-JETP 33, 1053 (1971).
[36]P. Lawaetz, Phys. Rev. B 4, 3460 (1971).
[37]G. Fishman, These d'Etat (Orsay, 1974)(unpublished). We wish to thank G. Lampel for calling this work to our attention and pointing out its potential applicability to our problem.
[38]D. M Campbell, H. M. Brash, and P. S. Farago, Phys. Lett A 36, 449 (1971).
[39]J. H. Pollard, *Second European Electro-Optics Markets and Technology Conference, Montreux, Switzerland, 1974* (Mack-Brook Exhibitions, Ltd., St. Albans, 1975).
[40]L. W. James and J. L. Moll, Phys. Rev. 183, 740 (1969).
[41]An increased polarization in the luminescence experiment has been predicted when there is a preferred axis in the distribution of the photoholes. M. I. Dyakanov and V. I. Perel, Sov. Phys.-Semicond. 7, 1551 (1974).
[42]R. R. L. Zucca, J. P. Walter, Y. R. Shen, and M. L. Cohen, Solid State Commun. 8, 627 (1970).
[43]F. H. Pollak and M. Cardona, Phys. Rev. 172, 816 (1968).
[44]U. Heinzmann, K. Jost, J. Kessler, and B. Ohnernus, Z. Phys. 251, 354 (1972).
[45]K. Koyama and H. Merz, Z. Phys. B 20, 131 (1975).
[46]V. W. Hughes, in *Proceedings of the Fifth International Conference on High Energy Accelerators* (Comitato Nazionale per l'Energia Nucleare, Rome, Italy, 1966), p. 531.
[47]B. Bederson, Comments At. Mol. Phys. 1, 41 (1969).
[48]C. E. Kuyatt and J. A. Simpson, Rev. Sci. Instrum. 38, 103 (1967).
[49]V. W. Hughes, R. L. Long, Jr., M. S. Lubell, M. Posner, and W. Raith, Phys. Rev. A 5, 195 (1972).
[50]Note that it is not always possible to trade off P and I. The maximum I may be limited as, for example, in high-energy polarized-electron scattering from a polarized-proton target, where target degradation limits the tolerable beam current. The minimum P may also be limited by noise or systematic uncertainties of a measurement.
[51]J. H. Pollard, *Second European Electro-Optics Markets and Technology Conference, Montreux, Switzerland, 1974* (Mack-Brook Exhibitions, Ltd., St. Albans, 1975).
[52]J. Kessler, in *Atomic Physics 3*, edited by J. Smith and G. K. Walters (Plenum, New York, 1973), p. 523. K. Jost, in *Physics of Ionized Gases 1972*, edited by M. V. Kurepa (Institute of Physics, Beograd, 1972).
[53]M. J. Alguard *et al.*, *Ninth International Conference on High Energy Accelerators*, (National Technical Information Service, Washington, D. C., 1975), p. 313; Bull. Am. Phys. Soc. 21, 35 (1976).
[54]P. S. Cooper *et al.*, Phys. Rev. Lett. 34, 1589 (1975).
[55]W. v. Drachenfels, U. T. Koch, R. D. Lepper, T. M. Müeller, and W. Paul, Z. Phys. 269, 387 (1974).
[56]P. J. Keliher, R. E. Gleason, and G. K. Walters, Phys. Rev. A 11, 1279 (1975).
[57]N. Müller, W. Eckstein, W. Heiland, and W. Zinn, Phys. Rev. Lett. 29, 1651 (1972).
[58]M. Wilmers, R. Haug, and H. Deichsel, Z. Angew. Phys. 27, 204 (1969).
[59]J. Kessler, Rev. Mod. Phys. 41, 3 (1969).
[60]C. J. Davisson and L. H. Germer, Phys. Rev. 33, 760 (1929).
[61]C. E. Kuyatt, Phys. Rev. B 12, 4581 (1975). Davisson

and Germer actually observed a spin polarization of ~15% in a double-scattering experiment with Ni crystals. They used the polarization of light as the model for their data analysis and therefore looked for a second harmonic in the variation of electron scattering with the angle of rotation of the second crystal, instead of the first harmonic, which gives the spin polarization.

[62]M. R. O'Neill, M. Kalisvaart, F. B. Dunning, and G. K. Walters, Phys. Rev. Lett. 34, 1167 (1975).
[63]E. Garwin (private communication).
[64]R. Celotta (private communication).